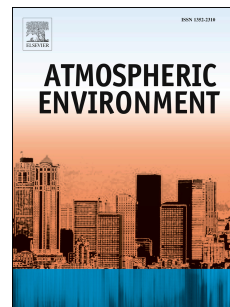


Journal Pre-proof

Online characterization of a large but overlooked human excreta source of ammonia in China's urban atmosphere

Sheng-Cheng Shao, Yan-Lin Zhang, Yun-Hua Chang, Fang Cao, Yu-Chi Lin, Ahsan Muzaffar, Yi-Hang Hong



PII: S1352-2310(20)30196-5

DOI: <https://doi.org/10.1016/j.atmosenv.2020.117459>

Reference: AEA 117459

To appear in: *Atmospheric Environment*

Received Date: 16 September 2019

Revised Date: 30 March 2020

Accepted Date: 31 March 2020

Please cite this article as: Shao, S.-C., Zhang, Y.-L., Chang, Y.-H., Cao, F., Lin, Y.-C., Muzaffar, A., Hong, Y.-H., Online characterization of a large but overlooked human excreta source of ammonia in China's urban atmosphere, *Atmospheric Environment* (2020), doi: <https://doi.org/10.1016/j.atmosenv.2020.117459>.

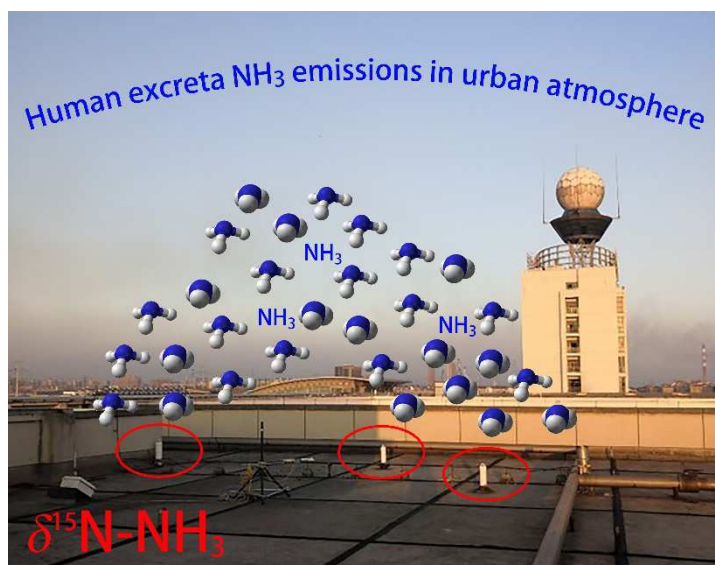
This is a PDF file of an article that has undergone enhancements after acceptance, such as the addition of a cover page and metadata, and formatting for readability, but it is not yet the definitive version of record. This version will undergo additional copyediting, typesetting and review before it is published in its final form, but we are providing this version to give early visibility of the article. Please note that, during the production process, errors may be discovered which could affect the content, and all legal disclaimers that apply to the journal pertain.

© 2020 Published by Elsevier Ltd.

Credit Author Statement

YZ designed the study. SS, YH and YC performed the research. SS analyzed the data. SS, YL and YC wrote the paper, with inputs from YZ, FC, AM.

Journal Pre-proof



TOC art

1 **Online characterization of a large but overlooked human excreta**
2 **source of ammonia in China's urban atmosphere**

3 **Sheng-Cheng Shao**^{1,2}, **Yan-Lin Zhang**^{1,2}, **Yun-Hua Chang**^{1,2}, **Fang Cao**^{1,2},
4 **Yu-Chi Lin**^{1,2}, **Ahsan Muzaffar**^{1,2}, **Yi-Hang Hong**^{1,2}

5 ¹ *Yale-NUIST Center on Atmospheric Environment, International Joint Laboratory on*
6 *Climate and Environment Change (ILCEC), Nanjing University of Information*
7 *Science & Technology, Nanjing 210044, China*

8 ² *Key Laboratory of Meteorological Disaster, Ministry of Education (KLME)/*
9 *Collaborative Innovation Center on Forecast and Evaluation of Meteorological*
10 *Disasters (CIC-FEMD), Nanjing University of Information Science & Technology,*
11 *Nanjing 210044, China*

12 Correspondence : Yan-Lin Zhang (zhangyanlin@nuist.edu.cn,
13 dryanlinzhang@outlook.com)

14
15 **ABSTRACT**

16 In urban China, human excreta are mostly stored in septic tanks beneath various
17 buildings, and the generated NH₃ are emitted to the atmosphere through ceiling ducts
18 on rooftops. Here we performed highly time-resolved measurements of NH₃
19 concentrations and auxiliary parameters in the ceiling duct of a typical building

20 complex during different seasons with varying temperature and population, allowing
21 an in-depth investigation of the driving forces in terms of governing NH₃ emissions.
22 Extremely high levels of NH₃ concentration (1013±793 μg m⁻³) were observed
23 throughout the campaign. Seasonally, the NH₃ concentration during summer vacation
24 (1377±1072 μg m⁻³) was significantly higher than during school time in fall (796±432
25 μg m⁻³) and winter (661±267 μg m⁻³). Moreover, the diurnal variation of NH₃ during
26 summertime was highly correlated with temperature ($R^2=0.95$, $p<0.01$), while it was
27 not the case for school time with dense population ($R^2=0.47$, $p<0.01$, $R^2=0.57$, $p<0.01$
28 in fall, winter, respectively). The highest temperature was 35.9 °C, with an emission
29 intensity peak of 4.1 mg s⁻¹ while the lowest temperature was 1.3 °C with an emission
30 intensity of 0.8 mg s⁻¹. The nitrogen stable isotopic composition of NH₃(δ¹⁵N-NH₃)
31 may be a useful tool to trace NH₃ sources. Here we report the δ¹⁵N-NH₃ measured
32 from ceiling duct collected directly, which constrains human excreta source δ¹⁵N-NH₃
33 values ($mean_{min}^{max}$) ‰ to $-35.6‰$ to $-31.9‰$ to $-39.8‰$. These results support that temperature is
34 the key factor in controlling NH₃ emissions from human excreta and demonstrate the
35 importance of using human excreta emitted δ¹⁵N-NH₃ to quantify excreta NH₃
36 contribution in urban atmospheres. Our findings highlight opportunities to limit NH₃
37 emissions from human excreta that will bring co-benefits to the air quality and human
38 health in urban China.

39 **Key words:** human excreta; ammonia; seasons; emission intensity; isotopic signature

40 1 Introduction

41 Gaseous ammonia (NH_3) is the most abundant alkaline gas in the atmosphere. It can
42 be released into the environment from both agricultural and non-agricultural sources.
43 Agricultural NH_3 sources mainly include fertilizer application and livestock
44 production, accounting for over 80 % of the global NH_3 emissions(He et al., 2011;
45 Vitousek et al., 2008). Despite the dominant role of agricultural NH_3 at global or
46 regional scales, non-agricultural NH_3 with miscellaneous sources (e.g., on-road
47 traffic(Chang et al., 2016b; Nowak et al., 2010; Pandolfi et al., 2012), urban green
48 land(Chan and Yao., 2008), NH_3 slips from coal-fired power plants(Pan et al., 2018),
49 wastewater(Häni et al., 2018; Yin et al., 2010) and solid waste(Häni et al., 2018))
50 exert disproportionately important contributions to the total NH_3 emissions of urban
51 areas. Although non-agricultural sources contribute a small part of the global NH_3
52 emissions, they are more locally concentrated, particularly on an urban scale. Besides,
53 urban areas are generally featured with NO_x and SO_2 rich atmospheres, gaseous NH_3
54 partitions is transformed into aerosol phase by reacting with sulfuric and nitric acids;
55 then forms ammonium nitrate (NH_4NO_3), ammonium sulfate ($(\text{NH}_4)_2\text{SO}_4$), and
56 ammonium bisulfate (NH_4HSO_4), which are major chemical component of fine
57 particulate matter ($\text{PM}_{2.5}$) (An et al., 2019; Butler et al., 2016; Durbin et al., 2002; Su
58 et al., 2016).

59 A lot of evidence suggests that nonagricultural activities like wastewater treatment
60 (Pennisi et al.,2012; Guo et al., 2020), coal combustion (Fan et al., 2019), solid
61 garbage (Hironori et al., 2011), vehicular exhaust (Zhang et al., 2020), and urban

62 green space are also important sources to ambient NH_3 . For example, the emission
63 rate of NH_3 from vehicle exhaust was 1300 tons in Shanghai in 2014, which
64 accounted 12% of total NH_3 emissions in this mega-city (Chang et al., 2019). Yao et
65 al. (Yao et al 2008) suggests that NH_3 from vehicular emissions can be neglected and
66 they proposed that urban green spaces are the dominant contributor to urban
67 atmospheric NH_3 in North American and Northern China. On the other hand,
68 volatilization of digested sludge is another important source of atmospheric NH_3 ,
69 which accounts for 27% of the total NH_3 emissions in England. Sutton et al. (Sutton et
70 al., 2000) considered NH_3 emission under sludge injection as 75% less than spreading.
71 In addition, Pan et al.(Pan et al., 2018) suggests that coal-fired power plants is an
72 crucial source of NH_3 at urban site with a contribution as high as 16%. This clearly
73 indicates that the non-agricultural emissions and sources of NH_3 deserve a more
74 comprehensive discussion in the scientific community.

75 It has been documented that NH_3 emissions from human excrement exist all over
76 the world(Chang et al., 2015; Sutton et al., 2000), and in most developed countries,
77 including their rural areas(Healy et al., 1970; Williams, 2005). But unlike Europe or
78 the U.S, human excrements are mostly stored in septic tanks beneath various
79 buildings in Chinese cities. Human excrements that are stored in septic tanks are not
80 directly discharged into sewer pipes, but are discharged into the atmosphere through a
81 ceiling duct connected to the roof(Driscoll et al., 2003). Therefore, human excrements
82 from urban buildings in China may be a significant source of NH_3 emission. As a

83 product of microbial decomposition in septic tanks due to prolonged septic tanks, a
84 large amount of gas (including NH_3) in the septic tank is directly released into the
85 atmosphere through the ceiling duct on the roof. This unique and potentially
86 important source of NH_3 in Chinese cities has received little attention in previous
87 studies (Chang et al., 2015).

88 The application of stable nitrogen (N) isotopes as a potential tracer of origin of NH_3
89 has been proposed (Elliott et al., 2019), which might help constrain regional NH_3
90 budgets. Zhang et al. (2007) has been proven very helpful for characterizing NH_3
91 emission sources (Chang et al., 2016a; Felix et al., 2013b; Ti et al., 2018). For
92 example, field-observed $\delta^{15}\text{N}$ signatures of NH_3 emitted from volatility-driven
93 sources (i.e., -31.7‰ to -27.1‰, -30.8‰ to -26.9‰, and -51.2‰ to -47.1‰ for
94 livestock, waste, and fertilizer) are distinct from combustion-related sources (i.e.,
95 -10.21‰ to 0.20‰), highlighting the potential of N isotope measurements to trace
96 agricultural versus non-agricultural NH_3 emission sources, especially in urban
97 areas (Chang et al., 2016a; Chang et al., 2019a; Felix et al., 2017). One challenge,
98 however, is that the large variability of the observed $\delta^{15}\text{N-NH}_3$ values, may partly
99 reflect the influence of atmospheric processes (not solely the emissions source) that
100 are associated with N isotope fractionation (Walters et al., 2019; Walters and Hastings,
101 2018). Indeed, once released into the atmosphere, NH_3 undergoes a number of
102 potential physical (e.g., deposition) and chemical processes (e.g., particle nucleation
103 and condensation) that can alter their primary isotopic “fingerprints” and the isotopic

104 composition of their reaction products (e.g., aqueous and solid NH_4^+)(Altieri et al.,
105 2014; Asman et al., 1998; Hastings et al., 2013; Xiao et al., 2012).

106 NH_3 can be detected by both active and passive sampling (Anderson et al., 2013;
107 Chang et al., 2016b; Meng et al., 2011; Ru-Jin et al., 2014; Wentao et al., 2011).
108 Previously, passive sampling methods have reported extremely high concentrations of
109 NH_3 in the ceiling ducts of various buildings in the urban areas(Chang et al., 2015).
110 However, the emission mechanism behind those high concentrations and the emission
111 intensity have not been carefully studied. The current passive sampling methods
112 suffer from several weaknesses including but not limited to low time resolution. The
113 collected passive samples cannot be stored for a long time because of contamination
114 (M.J Roadman, et al., 2003). To this end, this study uses an online instrument that is
115 capable of continuously monitoring NH_3 concentrations emitted from the ceiling duct,
116 with high time resolution (1 hour) and a high degree of accuracy.

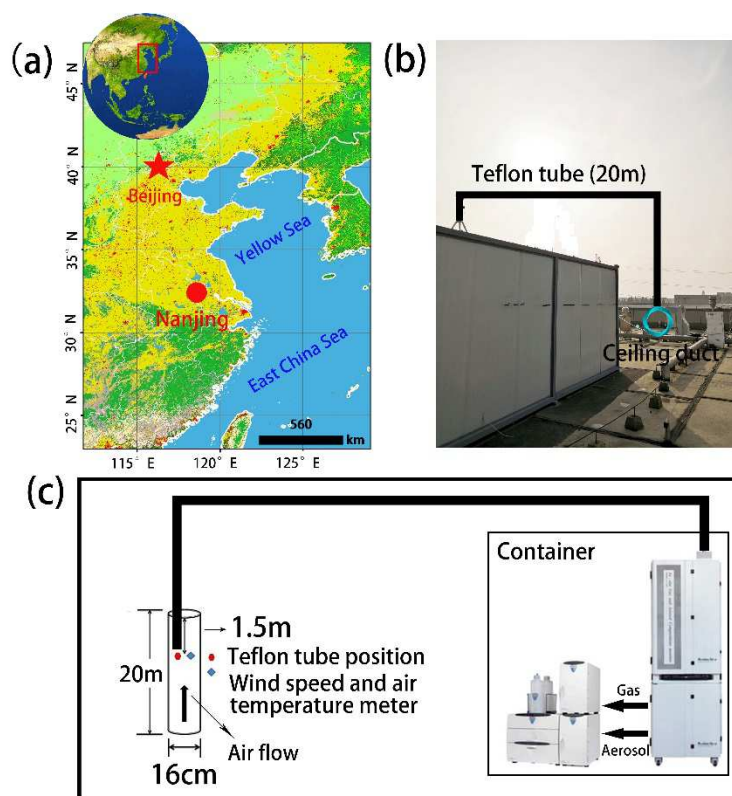
117 In this research, a typical ceiling duct in a teaching building with varying
118 population and temperature are selected to thoroughly investigate its NH_3 emission
119 characteristics and potential driving factors. During the summer vacation, there are
120 fewer human activities in the teaching building and temperature is much higher
121 compared to those of school time. This study aims at clarifying the relationships
122 between the different factors and providing a theoretical basis for clearing NH_3

123 emission channels of Chinese characteristics and quantifying the atmospheric human
124 excreta sources of NH_3 in urban atmospheres.

125 **2 Materials and methods**

126 **2.1 Site description**

127 Measurements of human excreta-emitted NH_3 were performed in a ceiling duct on
128 the rooftop of a six-floor teaching building in Nanjing (Fig. 1a), a typical megacity in
129 eastern China. The teaching building (Wendelou or WDL in short; 32.20°E ,
130 118.42°N) is located on the campus of Nanjing University of Information Science and
131 Technology (NUIST), which has 248 classrooms, 62 toilets, and 1 septic tank (60 m^3
132 in volume). The septic tank for human excreta was built in the bottom of WDL. In
133 total, there are four ceiling ducts (16 cm in diameter and length about 20 m) on the
134 rooftop, connected with the septic tank. (Fig. 1b).



135

136 **Figure 1.** The location of Nanjing city (a). Field picture of instruments set-up on

137 the rooftops of WDL (b). A sketch of the collection between ceiling duct and IGAC

138 instrument (c).

139 **2.2 NH₃ measurements**

140 The sampling campaign was conducted from July to December 2018. The hourly

141 NH₃ measurements in the ceiling duct were divided into three periods, i.e., vacation

142 time in summer (14/7 14:00 to 20/7 19:00; high temperature and almost no people),

143 school time in fall (6/9 12:00 to 17/9 9:00; relatively low temperature and dense

144 population), and school time in winter (6/12 10:00 to 8/12 12:00; very low

145 temperature and dense population), with the aim to identify the driving forces

146 controlling NH₃ emissions from human excreta. As a comparison, ambient NH₃

147 concentrations were also measured during three periods, i.e., 1:00 21/7 to 9:00 27/7,
148 1:00 18/9 to 1:00 28/9, and 19:00 2/12 to 23:00 4/12.

149 Hourly NH_3 concentrations were measured by an In-situ Gas and Aerosol
150 Compositions monitor (IGAC; Fortalice International Co; Taiwan). Specifically, the
151 IGAC platform is composed of three subsystems: a particle collection unit, an annular
152 denuder, and an ion chromatograph analyzer (IC)(Tian et al., 2017). Air was pumped
153 into a sharp-cut cyclone operating at a flow rate of 16.7 L min^{-1} . The air was drawn
154 through the annular denuder which wetted with dilute H_2O_2 solution. The
155 aerosol-collecting device, a Rapid Capture Fluid Particle (PCFP), was placed
156 downstream of the denuder. It employs the mechanism of wet scrubbing, particle
157 condensation growth, and impaction to capture particles. The gas and aerosol liquid
158 extracts from denuder and PCFP are subsequently injected into the two ICS once an
159 hour for cations and anions. Since the sampling Teflon tube was directly placed into
160 the exhaust vent of the ceiling duct (see in Figure S2), the interference of the ambient
161 air is eliminated. The NH_4^+ concentration is a low in the pre-experiment so it ignored
162 here. The performance of IGAC has been widely validated in previous work(Chang et
163 al., 2007; Young et al., 2016).

164 The exhaust vent of the ceiling duct and the $\text{PM}_{2.5}$ cutting head of the IGAC were
165 connected by a Teflon tube (6.5 mm in diameter and length about 20 m) (Fig 1c). To
166 avoid potential interference from the ambient atmosphere, the Teflon tube was
167 inserted into the exhaust tube (1.5 m in length). The sampling site of the ambient

168 atmosphere is located at the same location (Figure S1 and Figure S2). The cutting
169 head is transformed into the sampling of the ambient atmosphere, and the system was
170 cleaned once after the transformation.

171 Meteorological parameters including relative humidity, temperature, wind speed, and
172 wind direction, were hourly observed by a co-located Met station one (HMP155 U.S)
173 at the same building.

174 **2.3 NH₃ emission intensity**

175 The NH₃ emission intensity (EI) is the mass of the substance discharged per unit
176 time. Since the concentration in the ceiling duct is greater than the concentration in
177 the ambient atmosphere and the septic tank is constantly releasing gas, the ceiling
178 duct can be regarded as a one-way passage of NH₃ from the septic tank to the ambient
179 atmosphere. The amount of NH₃ discharged from the septic tank to the ambient
180 atmosphere via the ceiling duct per unit time is expressed in mg hr⁻¹. Accordingly, the
181 EI based on the flow transmission flux can be established. Specifically, for a
182 particular building, the NH₃ EI of urban human settlements building is related to the
183 air flux (indicated by wind speed), sampling time, and NH₃ concentration in the
184 ceiling duct:

$$185 \quad EI = \pi \times r^2 \times C \times \frac{W \times 3.6 \cdot 10^3}{1 \cdot 10^3} \quad (1)$$

186 Where EI is the emission intensity (mg NH₃ hr⁻¹); r represents the inner diameter of
187 the ceiling duct (0.08 m); C represents hourly average NH₃ concentration in the

188 ceiling duct ($\mu\text{g m}^{-3}$); W stands for the wind speed (m s^{-1}) inside the ceiling duct;
189 $1 \cdot 10^3$ represents the coefficient of mass unit converted from μg to mg ; $3.6 \cdot 10^3$ is a
190 constant, which is converted from second to hour.

191 In order to quantify the discharge flux of the ceiling duct and calculate the emission
192 intensity, the WFWZY-1 universal wind speed recorder was also placed in the ceiling
193 duct (1.5 m from the exhaust vent; Fig. 1c) to measure the interior wind speed per
194 second. The accuracy of the measurements of wind speed is 0.01m s^{-1} .

195 **2.4 Nitrogen isotopic analysis**

196 A newly developed chemical method for $\delta^{15}\text{N-NH}_4^+$ of low NH_4^+ samples was used
197 in the current work. The detailed analytical procedures are given elsewhere (Liu et al.,
198 2014). Briefly, this method is based on the $\delta^{15}\text{N}$ isotopic analysis of N_2O , which is
199 much less abundant in the atmosphere than N_2 and thus causes minimal atmospheric
200 contamination. The filtered samples were firstly extracted with ultra-pure water (18.2
201 $\text{M}\Omega \text{ cm}$). Concentrations of NH_4^+ were then analyzed using an ion chromatographic
202 system (883 Basic IC plus, Metrohm Co., Switzerland) equipped with a Metrosep
203 C4/4.0 cation column. In this analysis, we used $1.0 \text{ mmol L}^{-1} \text{HNO}_3 + 0.5 \text{ mmol L}^{-1}$
204 pyridine dicarboxylic acid as eluent and the detection limit of NH_4^+ was 0.0028 mg
205 L^{-1} . After the measurement of the NH_4^+ concentration, the extracted sample was
206 oxidized to NO_2^- by hypobromite (BrO^-) in a vial. NO_2^- was then quantitatively
207 converted into N_2O by hydroxylamine (NH_2OH) under strongly acid conditions. The

208 produced N₂O was subsequently analyzed $\delta^{15}\text{N}$ - N₂O by a purge and cryogenic trap
 209 system (Gilson GX-271, IsoPrime Ltd., Cheadle Hulme, UK) coupled to an IRMS
 210 (PT-IRMS) (IsoPrime 100, IsoPrime Ltd., Cheadle Hulme, UK) at the Yale-NUIST
 211 Isotope Atmoschemistry Lab for N isotopic analysis within one month.

212 Isotope ratio values are reported in parts per thousand relatives to atmospheric N₂ as
 213 follows:

$$214 \quad \delta^{15}\text{N}(100\%) = \frac{(^{15}\text{N}/^{14}\text{N})_{\text{sample}} - (^{15}\text{N}/^{14}\text{N})_{\text{N}_2}}{(^{15}\text{N}/^{14}\text{N})_{\text{N}_2}} \times 1000 \quad (2)$$

215 Three international standards (IAEA N1, USGS 25, and USGS26 with $\delta^{15}\text{N}$ values
 216 of +0.4, -30.4, and +53.7 ‰, respectively) were used to correct the reagent blank and
 217 drift during isotope analysis. The standard deviation of $\delta^{15}\text{N}$ measurements is less
 218 than 0.3 ‰.

219 To minimize isotope fractionation of $\delta^{15}\text{N}$ -NH₃ during the sampling process, an active
 220 sampling method was used to collect NH₃ samples from the ceiling duct emission
 221 source. Due to the high concentration of emission sources, active sampling
 222 (absorption efficiency is close to 100%) was conducted from the source to avoid
 223 interference from the external environment. In the preliminary experiment, the other
 224 ion concentration was lower than the blank approximation, which can be ignored.
 225 Therefore, this method also applies to the collection of vehicle exhaust, biomass
 226 combustion and other samples (Pan et al 2018, Chang et al 2016). On the other hand,

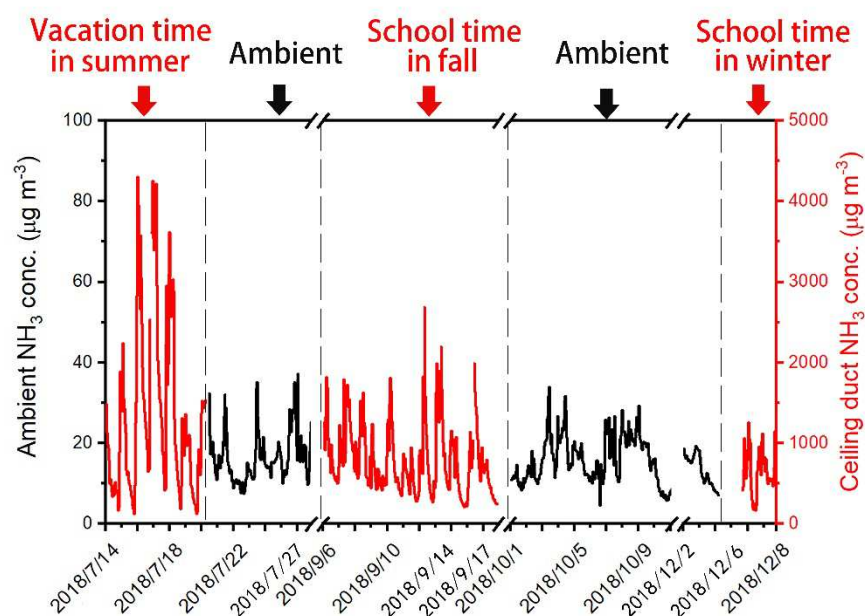
227 human excreta samples were collected using a modified version of the United States
228 Environmental Protection Agency (US EPA) Method 7. Briefly, human excreta
229 samples were collected by a double-pneumatic air sampler (flow rate $\sim 2 \text{ L min}^{-1}$),
230 which contain two 25 ml borosilicate bottles. When collection NH_3 samples emitted
231 from the ceiling duct, the sampler was placed near the exit ($\sim 1.5\text{m}$) of the ceiling duct
232 and each sampling was conducted for 2 hours in summer (i.e., 6:00-8:00, 12:00-14:00,
233 18:00-20:00, for three days; $n=9$) and winter (i.e., 6:00-8:00, 12:00-14:00,
234 18:00-20:00, for two days; $n=6$). The sampling bottles contained $15 \text{ mL } 0.05 \text{ mol L}^{-1}$
235 H_2SO_4 as NH_3 absorbing solution. During the sampling process, NH_3 would be
236 absorbed by acidic solution. After sampling, the samples were sent back to the
237 laboratory and conditioned for 5 days. During the conditioned process, the samples
238 have to be shook 3-5 times per day to facilitate the conversion of NH_3 to NH_4^+ . After
239 that, the NH_4^+ concentration in the absorbing solution was determined using an ion
240 chromatography (Thermo Fisher Scientific, Sunnyvale, USA) and the $\delta^{15}\text{N}$ were
241 analyzed by the IRMS as mentioned above.

242 **3 Results and discussion**

243 **3.1 Human excreta as an important NH_3 source to influence ambient NH_3**

244 As depicted in Fig. 2, 863 hourly NH_3 concentrations were successfully measured
245 throughout the sampling campaign, 449 and 414 were measured inside and outside the
246 ceiling duct, respectively. The NH_3 concentrations ($\text{mean}_{\text{min}}^{\text{max}} \pm 1\sigma$) we measured in

247 the ceiling duct ($1013 \frac{4304.9}{123.6} \pm 793 \mu\text{g m}^{-3}$) were two to three orders of magnitude
 248 higher than that of the ambient air ($15.6 \frac{37.2}{4.6} \pm 5.6 \mu\text{g m}^{-3}$), indicating that human
 249 excreta are an important source of NH_3 . Our results are consistent with Chang et al.
 250 (2015) that also reported extremely high concentrations of NH_3 in the ceiling ducts of
 251 various buildings across Shanghai ($1128 \frac{5937.0}{148.0} \pm 404 \mu\text{g m}^{-3}$ in summer). Given
 252 that septic tanks are a dominant sanitation system in urban China, human excreta thus
 253 can be regarded as a ubiquitous NH_3 source in China's urban atmospheres.



254
 255 **Figure 2.** The overall change in NH_3 concentration (yyyy/mm/dd) (Red is the NH_3
 256 concentration in the ceiling duct, blank represent the NH_3 concentration on ambient).

257

258 Using a variety of chemical, physical, and optical techniques, there is an increasing
 259 number of studies in terms of investigating the influences of NH_3 source emissions
 260 (e.g., livestock waste, fertilizer application, traffic, industrial processes) on ambient

261 NH₃ concentrations in China (Table 1). Although the main source of NH₃ is
 262 agriculture, field monitoring results in Table 1 show that the concentrations of NH₃ in
 263 urban areas are generally higher than that in rural areas, indicating that urban areas are
 264 a hot spot of NH₃ emissions. In the present study, the average ambient NH₃
 265 concentration (mean±1σ) measured at WDL was 15.6±5.6 μg m⁻³, which is not only
 266 higher than all the sites in rural areas but higher than most sites in urban areas.
 267 Previous studies suggested that on-road traffic and NH₃ slip from the coal-fired power
 268 plant are the major non-agricultural sources contributing to the high levels of NH₃ in
 269 urban atmospheres. However, both performed in Nanjing, our measured NH₃
 270 concentration at WDL was much higher than that measured in downtown area (Pan et
 271 al., 2018; Wang et al., 2016; Zheng et al., 2015). Moreover, the NH₃ concentrations
 272 measured at the roadside and industrial sites were less than half of our measured NH₃
 273 concentration. We thus infer that the high NH₃ concentration at WDL can be
 274 attributed to the strong influence of NH₃ emissions from the ceiling duct.

275

276 **Table 1.** Ambient NH₃ concentration measurements in China

Location	Period	Land use types	methodology	Time resolution	NH ₃ (μg m ⁻³)	Reference
WDL, Nanjing	7-12/2018	urban	IGAC	hourly	15.6±5.6	This study
Nanjing	6-7/2015	urban	MARGA	monthly	9.5	(Pan et al., 2018)
Nanjing	8-11/2012	urban (near industrial)	HRTOF-CIMS	1 Hz	1.3±1.8	(Zheng et al., 2015)

Nanjing	7-8/2013	urban (near road)	Portable NH ₃ online detector	Hourly	6.7	(Wang et al., 2016)
Beijing	2/2009-7/2009	urban	Ogawa	weekly	18.1±13.8	(Meng et al., 2011)
Shanghai	4/2014-7/2015	urban	MARGA	weekly	6.4±2.3	(Chang et al., 2019b)
Guangzhou	11/2010	urban	OP-DOAS	2.5 min	1.6	(Wang et al., 2012)
Guangzhou	9-11/2015	urban	Diffusive sampler	monthly	4.9	(Pan et al., 2018)
Shanghai	4/2014-4/2015	urban	MARGA	hourly	5.6±3.9	(Chang et al., 2016a)
Tianjin	6-8/2015	urban	Diffusive sampler	monthly	14.5	(Pan et al., 2018)
Chengdu	6-8/2015	urban	Diffusive sampler	monthly	10.5	(Pan et al., 2018)
Xian	4/2006-4/ 2007	urban	Ogawa	daily	12.9	(Zhang et al., 2002)
Huanjiang	2-3/2015	background	Diffusive sampler	monthly	3.6	(Pan et al., 2018)
Changzhou	2-3/2015	suburban	Diffusive sampler	monthly	6.0	(Pan et al., 2018)
Linze	3-5/2015	rural	Diffusive sampler	monthly	3.7	(Pan et al., 2018)
Beijing	8-9/2015	rural	ALPHA	daily	14.0±1.6	(Xu et al., 2015)
Shanghai	4/2014-7/2015	rural	MARGA	weekly	5.1±3.1	(Chang et al., 2019b)
Linyi	8-12/2015	rural	ALPHA	daily	5.5	(Xu et al., 2015)
Baoding	8-12/2015	rural	ALPHA	daily	11.8	(Xu et al., 2015)

277

278 **3.2 Driving factors in controlling NH₃ concentrations in the ceiling duct**

279 In order to further understand the driving factors controlling NH₃ emissions in the
 280 ceiling duct, the whole sampling campaign was divided into three periods with
 281 varying temperature and population to compare their NH₃ concentrations and
 282 emission rates. The time-series variations of NH₃ concentrations in and out of the
 283 ceiling duct during different periods are illustrated in Figure 2, in which most NH₃
 284 concentration spikes were concentrated in the summertime. Specifically, the highest
 285 NH₃ concentration (4304.9 µg m⁻³) has occurred 17/7 12:00 when temperature also
 286 reached at a very high level (37 °C). During summer vacation, apart from the on-duty
 287 staff, there were almost no other people to use the toilet. Thus, NH₃ emissions in this
 288 period were largely driven by temperature rather than human activities. In Table 2, the
 289 descriptive statistics of all measured parameters in different periods are reported, in
 290 which the average NH₃ concentrations both in and out of the ceiling duct were the
 291 highest during summer, followed by that during fall and winter. This is also the case
 292 for NH₃ emission intensity in the ceiling duct and ambient temperature. These results
 293 highlight the importance of temperature in terms of controlling NH₃ emissions from a
 294 ceiling duct.

295 **Table 2.** Comparison of NH₃ concentration and temperature in and out of the
 296 ceiling duct during different periods.

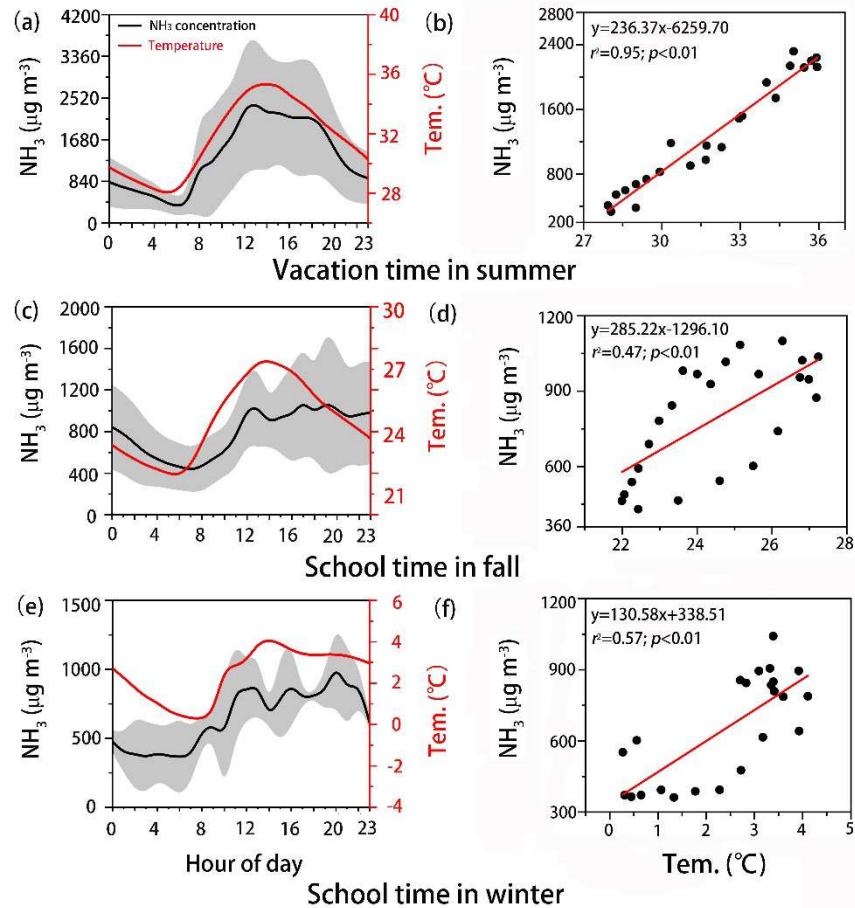
	Time	T (□)	NP ^a	NH ₃ (µg m ⁻³)	N ^b	EI ^c (mg hr ⁻¹)
Vacation in summer	2018.7.14 13:00-					
	Ceiling duct	31.8±2.8	1-2	1377±1072	151	3.6±1.8
	2018.7.20 19:00					

	Ambient	2018.7.21 1:00- 2018.7.27 9:00	30.1±2.8	/	17±7	151	/
School time	Ceiling duct	2018.9.6 12:00- 2018.9.17 9:00	24.5±2.3	1000- 1200	796±432	247	2.5±1.3
	Ambient	2018.10.1 1:00- 2018.10.11 1:00	21.1±3.2	/	16±6	212	/
School time	Ceiling duct	2018.12.6 10:00- 2018.12.8 12:00	2.4±2.5	1000- 1200	661±267	51	2.2±1.1
	Ambient	2018.12.2 19:00- 2018.12.4 23:00	11.7±2.6	/	12±3	53	/

297 Notes: a: Estimated number of people at the WDL. b: The number of samples. c: Emission intensity

298 In our study, hourly observations of NH₃ concentrations in the ceiling duct over
 299 long-term periods offer a unique opportunity to provide robust diurnal profiles, which
 300 can be used to further examine the effects of natural and anthropogenic factors in
 301 terms of influencing NH₃ emissions. Figure 3 depicts the diurnal variations of NH₃
 302 concentration and temperature measured during different periods in the ceiling duct.
 303 Different from the results measured during fall and winter, the diurnal profile of NH₃
 304 concentration during summer shows a unimodal variation, with the maximum
 305 occurred on 13:00 (Fig. 3a), which is generally consistent with the variation of
 306 temperature. Indeed, Fig. 3b reveals that, NH₃ concentrations in the ceiling duct were

307 highly correlated with temperature ($r^2 = 0.95$), confirming that without the
 308 interference of people using the toilet, the temperature is almost the only factor in
 309 terms of controlling NH_3 emissions from human excreta during summertime.



310

311 **Figure 3.** Diurnal variations of the average NH_3 in the ceiling duct and ambient
 312 temperature and their correlation analysis during vacation in summer (a and b), school

313 time in fall (c and d), and school time in winter (e and f) (the gray shaded area

314 represent the range of observed values during each period).

315

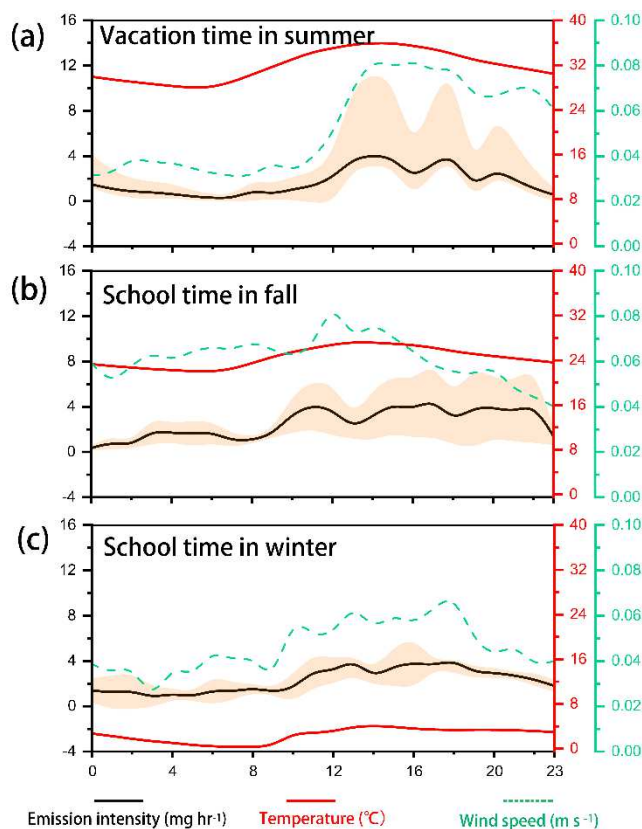
316 Correlation analysis between NH_3 concentration and temperature during fall (Fig.
317 3d) and winter (Fig. 3f) also suggest a potentially important influence of temperature.
318 However, increased from 8:00, their diurnal profiles of NH_3 characterized by
319 relatively flat variation at a high level during the afternoon. This can be explained the
320 intensive using of toilets during school time, indicating that human activities can be
321 another important factor in terms of controlling NH_3 emissions from human excreta.
322 Nevertheless, their NH_3 concentrations were still significantly lower than that during
323 summer. Therefore, the temperature is the most important factor in regulating NH_3
324 concentrations in the ceiling duct.

325 **3.3 Temperature-driven variability in NH_3 emission intensity**

326 As discussed above, NH_3 concentrations in the ceiling duct are mainly controlled by
327 temperature. However, NH_3 emission intensity (EI) is the function of NH_3
328 concentration and wind speed in the ceiling duct. Therefore, it is not clear if NH_3 EI is
329 also governed by temperature. Fig. 4 illustrates the diurnal profiles of NH_3 EI from
330 the ceiling duct, wind speed in the ceiling duct, and ambient temperature, during
331 different periods. Among the three periods, on the whole, the emission intensity of all
332 three seasons showed a trend of fluctuation and increase after 8:00 am, and gradually
333 decreased with the change of seasons. NH_3 EI varied within the largest ranges during
334 the vacation in summer (Fig. 4a), followed by the school time in fall (Fig. 4b) and
335 winter (Fig. 4c). Among each period, there was also a larger variation range during

336 daytime than during nighttime. As shown in figure 4, the correlation coefficients
337 between (R^2) emission intensity and temperature were 0.69 ($p<0.01$), 0.49 ($p<0.01$)
338 and 0.62 ($p<0.01$) in summer vacation, school time in fall and school time in winter,
339 respectively. Previous work has proven that temperature was an important factor that
340 effected NH_3 emission from waste slurries (Génermont, S., and P. Cellier et al., 1997),
341 wind speed on aerodynamic conductance (Roelle, P.A et al., 2002; Beuning, J.D et al.,
342 2008.) and the effects of temperature on volatilization through the Henry constant
343 (Montes, F et al., 2009). In this work, emissions peak of NH_3 (EI up to 4.1 mg s^{-1}) was
344 found at 13:00-15:00 in summer vacation. Meanwhile, higher levels of temperature
345 ($35.9 \text{ }^\circ\text{C}$) was also observed during this time. Thus, the high NH_3 EI was due to high
346 temperature, which was favorable for microbial activities in the septic tanks, leading
347 to more production of NH_3 . We estimated based on the emission intensity, these data
348 suggest that emissions of NH_3 from human excreta for urban population of ~8 million
349 people in Nanjing contribution 1289 Mg NH_3 annually to the atmosphere within the
350 city, which correspond to 8.9% of the total NH_3 emission in the Nanjing urban areas.

351



352

353 **Figure 4.** Emissions intensity comparison in Summer (a) /Fall(b)/Winter(c). Emission

354 intensity is calculated from the average hourly ammonia concentrations and wind speed

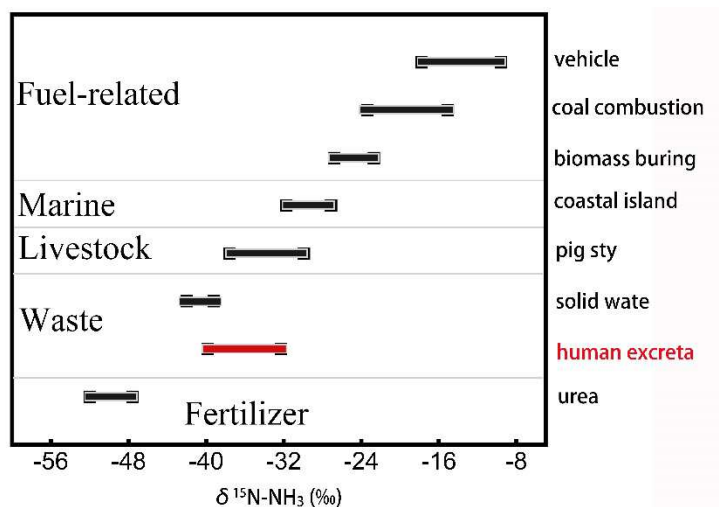
355 measured in the ceiling duct

356 **3.4 $\delta^{15}\text{N}$ values of human excreta NH_3** 357 Using $\delta^{15}\text{N}$ as a tool to discriminate the contribution of various sources to ambient358 NH_3 requires well-representative isotopic signatures of NH_3 emission sources. Direct359 ceiling duct measurements of human excreta allow us to evaluate $\delta^{15}\text{N}\text{-NH}_3$ without360 interference from other NH_3 sources. The $\delta^{15}\text{N}\text{-NH}_3$ from human excreta samples (15

361 in total) greatly varied from -39.8 to -32.3‰ in summer (n=9), -37.9 to -31.9‰ in

362 winter (n=6) where the NH_3 concentration ranged from 224 to 1450 $\mu\text{g m}^{-3}$, 321.3 to

363 $646.5 \mu\text{g m}^{-3}$ and the average $\delta^{15}\text{N}$ value ($\bar{x} \pm 1\sigma$) of ceiling duct emitted NH_3 was
 364 $-36.9 \pm 2.5\text{‰}$, $-33.7 \pm 2.2\text{‰}$, respectively. There is no significant correlation was
 365 found between $\delta^{15}\text{N}$ values and ambient temperature in summer ($R^2=0.18, P > 0.05$)
 366 and winter ($R^2=0.11, P > 0.05$), indicating that $\delta^{15}\text{N-NH}_3$ at the receptor site was not
 367 influenced by ambient temperature. In other words, the emission source (ceiling duct)
 368 was likely the main factor to control $\delta^{15}\text{N}$ in atmospheric NH_3 . The $\delta^{15}\text{N-NH}_3$ values
 369 of human excreta emissions collected in this study are similar to the livestock waste
 370 (Freyer, 2010; Hristov and Huhtanen, 2009; Lynch et al., 2006), Due to different
 371 sampling methodology, there may be differences in $\delta^{15}\text{N-NH}_3$. For different NH_3
 372 emission sources, the fluctuation of its $\delta^{15}\text{N-NH}_3$ is in a certain range (Figure 5)
 373 (livestock waste (-43‰ to -9‰)). NH_3 emitted from volatilized sources has relatively
 374 low $\delta^{15}\text{N}$ values, allowing them to be distinctly differentiated from NH_3 emitted from
 375 human excreta sources that are characterized by relatively high $\delta^{15}\text{N}$ values (Heaton,
 376 T.H et al., 1986).



377

378 **Figure 5.** The $\delta^{15}\text{N-NH}_3$ values in five different NH_3 emission sources. In this figure,
379 $\delta^{15}\text{N-NH}_3$ of human excreta are obtained in this work and others are acquired from the
380 literatures.

381 As a comparison, the $\delta^{15}\text{N}$ values of human exhaust and other various NH_3 sources
382 were compiled and their variation ranges are reported by Felix(Felix et al., 2013a).
383 These NH_3 sources can be classified into four categories based on their $\delta^{15}\text{N}$ values
384 and initial characteristics (Figure 5), i.e., fertilizer, waste, livestock, marine, and
385 fuel-related sources. The distribution of their variation ranges comes to a conclusion:
386 NH_3 emitted from vehicle exhausts has the highest $\delta^{15}\text{N}$ values, allowing them to be
387 distinctly differentiated from NH_3 emitted from other sources (especially
388 volatilization-related sources). Therefore, we confirm that ceiling duct measurements
389 of $\delta^{15}\text{N-NH}_3$ values can be ideally considered as the isotopic signature of human
390 excreta source. Collectively, the distinct $\delta^{15}\text{N}$ values of excreta-emitted NH_3
391 determined in this study can be used as a representative endmember of human excreta
392 source to discriminate the contribution of livestock waste to ambient NH_3 in urban
393 atmospheres.

394

395 **4 Conclusions**

396 This paper presents detailed results of NH_3 concentrations and auxiliary parameters
397 in the ceiling duct of a typical building complex during different seasons with varying

398 temperature and population. High concentrations of NH_3 were observed in and out of
399 the ceiling duct with high time resolution, confirming human excreta is a ubiquitously
400 important source of NH_3 in urban China and may strongly affect ambient NH_3
401 concentrations. Further studies found that the NH_3 concentration during summer
402 vacation ($1377 \pm 1072 \mu\text{g m}^{-3}$) was significantly higher than that of school time in fall
403 ($796 \pm 432 \mu\text{g m}^{-3}$) and winter ($661 \pm 267 \mu\text{g m}^{-3}$). Our findings show that temperature
404 as the most important factor in terms of controlling NH_3 concentrations in the ceiling
405 duct. This can be explained by the fact that a high temperature could facilitate the
406 microbial decomposition of human excreta in the ceiling duct. Furthermore, High
407 NH_3 emission intensity was also observed in the ceiling duct and mainly governed by
408 temperature. Using direct ceiling duct measurements, we shows that the amount of
409 NH_3 emission determines the expected range in $\delta^{15}\text{N-NH}_3$. Our approach constrains
410 human excreta source $\delta^{15}\text{N-NH}_3$ values ($mean_{min}^{max}$) to -35.6‰ – -31.9‰ – -39.8‰ . This result
411 particularly relevant for tracing sources and transport of NH_3 that contribute to
412 ammonium salt formation in urban environments. Given the importance of human
413 excreta-emitted NH_3 in China's urban areas, we urge the scientific community to
414 modify ceiling ducts so that they do not influence NH_3 measurements.

415

416 **Acknowledgements**

417 This study was financially supported by the National Key R&D Program of
418 China (Grant No. 2017YFC0210101), the Natural Scientific Foundation of China

419 (Grant No. 91644103), the Provincial Natural Science Foundation of Jiangsu (Grant
420 No. BK20180040), and Jiangsu Innovation and Entrepreneurship Team.

421

422 **References**

- 423 Altieri, K.E., Hastings, M.G., Peters, A.J., Oleynik, S., Sigman, D.M., 2014. Isotopic
424 evidence for a marine ammonium source in rainwater at Bermuda. *Global Biogeochem*
425 *Cy* 28, 1066-1080.
- 426 An, Z., Huang, R.-J., Zhang, R., Tie, X., Li, G., Cao, J., Zhou, W., Shi, Z., Han, Y., Gu,
427 Z., Ji, Y., 2019. Severe haze in northern China: A synergy of anthropogenic emissions
428 and atmospheric processes. *Proceedings of the National Academy of Sciences* 116,
429 8657-8666.
- 430 Anderson, J.S., Jonathan, R., Peters, J.C., 2013. Catalytic conversion of nitrogen to
431 ammonia by an iron model complex. *Nature* 501, 84.
- 432 Asman, W.A.H., Sutton, M.A., Schjorring, J.K., 1998. Ammonia: emission,
433 atmospheric transport and deposition. *New Phytol* 139, 27-48.
- 434 Bouwman, A.F., Lee, D.S., Asman, W.A.H., Dentener, F.J., Van, D.H., K. W, Olivier,
435 J.G.J., 1997. A global high-resolution emission inventory for ammonia. *Global*
436 *Biogeochemical Cycles* 11, 561-587.
- 437 Butler, T., Vermeylen, F., Lehmann, C.M., Likens, G.E., Puchalski, M., 2016.
438 Increasing ammonia concentration trends in large regions of the USA derived from the
439 NADP/AMoN network. *Atmospheric Environment* 146, 132-140.
- 440 Chan, C.K., Yao, X., 2008. Air pollution in mega cities in China. *Atmospheric*
441 *Environment* 42, 1-42.
- 442 Chang, S.Y., Lee, C.T., Chou, C.K., Liu, S.C., Wen, T.X., 2007. The continuous field
443 measurements of soluble aerosol compositions at the Taipei Aerosol Supersite, Taiwan.
444 *Atmospheric Environment* 41, 1936-1949.
- 445 Chang, Y., Deng, C., Dore, A.J., Zhuang, G., 2015. Human Excreta as a Stable and
446 Important Source of Atmospheric Ammonia in the Megacity of Shanghai. *PLoS One*
447 10, e0144661.
- 448 Chang, Y., Liu, X., Deng, C., Dore, A.J., Zhuang, G., 2016a. Source apportionment of
449 atmospheric ammonia before, during, and after the 2014 APEC summit in Beijing
450 using stable nitrogen isotope signatures. *Atmospheric Chemistry and Physics* 16,
451 11635-11647.
- 452 Chang, Y., Zou, Z., Deng, C., Huang, K., Collett, J.L., Lin, J., Zhuang, G., 2016b. The
453 importance of vehicle emissions as a source of atmospheric ammonia in the megacity of
454 Shanghai. *Atmospheric Chemistry and Physics* 16, 3577-3594.

- 455 Chang, Y., Zou, Z., Zhang, Y., Deng, C., Hu, J., Shi, Z., Dore, A.J., Collett, J., 2019a.
456 Assessing contributions of agricultural and non-agricultural emissions to atmospheric
457 ammonia in a Chinese megacity. *Environmental Science & Technology*.
- 458 Dragosits, U., Dore, A.J., Sheppard, L.J., Vieno, M., Tang, Y.S., Theobald, M.R.,
459 Sutton, M.A., 2008. Sources, Dispersion and Fate of Atmospheric Ammonia. *Nitrogen*
460 *in the Environment*, 333-393.
- 461 Driscoll, C.W.D., Aber, J., Boyer, E., Castro, M., Cronan, C., Goodale, C.L.,
462 Groffman, P., Hopkinson, C., Lambert, K., Lawrence, G., 2003. Nitrogen pollution in
463 the northeastern United States: Sources, effects, and management options [Review].
464 *Bioscience* 53, 357-374.
- 465 Durbin, T.D., Wilson, R.D., Norbeck, J.M., Miller, J.W., Tao, H., Rhee, S.H., 2002.
466 Estimates of the emission rates of ammonia from light-duty vehicles using standard
467 chassis dynamometer test cycles. *Atmospheric Environment* 36, 1475-1482.
- 468 Felix, J.D., Elliott, E.M., Gay, D.A., 2017. Spatial and temporal patterns of nitrogen
469 isotopic composition of ammonia at U.S. ammonia monitoring network sites.
470 *Atmospheric Environment* 150, 434-442.
- 471 Felix, J.D., Elliott, E.M., Gish, T.J., McConnell, L.L., Shaw, S.L., 2013a.
472 Characterizing the isotopic composition of atmospheric ammonia emission sources
473 using passive samplers and a combined oxidation-bacterial denitrifier approach. *Rapid*
474 *Communications in Mass Spectrometry* 27, 2239-2246.
- 475 Felix, J.D., Elliott, E.M., Gish, T.J., McConnell, L.L., Shaw, S.L., 2013b.
476 Characterizing the isotopic composition of atmospheric ammonia emission sources
477 using passive samplers and a combined oxidation-bacterial denitrifier approach. *Rapid*
478 *communications in mass spectrometry : RCM* 27, 2239-2246.
- 479 Freyer, H.D., 2010. Seasonal Trends of NH₄⁺ and NO₃⁻ Nitrogen Isotope
480 Composition in Rain Collected at Jülich, Germany. *Tellus* 30, 83-92.
- 481 Weidong Fan, Xiaofeng Wu, Hao Guo, Jiangtao Zhu, Peng Liu, Can Chen, Yong
482 Wang, Experimental study on the impact of adding NH₃ on NO production in coal
483 combustion and the effects of char, coal ash, and additives on NH₃ reducing NO under
484 high temperature, *Energy*, 2019, Pages 109-120.
- 485 Xiurui Guo, Zhilan Ye, Dongsheng Chen, Hongkan Wu, Yaqian Shen, Junfang Liu,
486 Shuiyuan Cheng, Prediction and mitigation potential of anthropogenic ammonia
487 emissions within the Beijing–Tianjin–Hebei region, China, *Environmental*
488 *Pollution*, 2020, 0269-7491.
- 489 Häni, C., Flechard, C., Neftel, A., Sintermann, J., Kupper, T., 2018. Accounting for
490 Field-Scale Dry Deposition in Backward Lagrangian Stochastic Dispersion Modelling
491 of NH₃ Emissions. *Atmosphere* 9, 146.
- 492 Hastings, M.G., Casciotti, K.L., Elliott, E.M., 2013. Stable Isotopes as Tracers of
493 Anthropogenic Nitrogen Sources, Deposition, and Impacts. *Elements* 9, 339-344.
- 494 He, J., Balasubramanian, R., Burger, D.F., Hicks, K., Kuylenstierna, J.C.I., Palani, S.,
495 2011. Dry and wet atmospheric deposition of nitrogen and phosphorus in Singapore.
496 *Atmospheric Environment* 45, 2760-2768.

- 497 Healy, T.V., McKay, H.A.C., Pilbeam, A., Scargill, D., 1970. Ammonia and
498 Ammonium Sulfate in the Troposphere over the United Kingdom. *Journal of*
499 *Geophysical Research* 75, 2317-2321.
- 500 Hristov, A.N., Huhtanen, P., 2009. Nitrogen efficiency in Holstein cows and dietary
501 means to mitigate nitrogen losses from dairy operations. *Proceedings*.
- 502 Liu, D., Fang, Y., Tu, Y., Pan, Y., 2014. Chemical method for nitrogen isotopic
503 analysis of ammonium at natural abundance. *Anal Chem* 86, 3787-3792.
- 504 Lynch, D.H., Voroney, R.P., Warman, P.R., 2006. Use of ^{13}C and ^{15}N natural abundance
505 techniques to characterize carbon and nitrogen dynamics in composting and in
506 compost-amended soils. *Soil Biology & Biochemistry* 38, 103-114.
- 507 Meng, Z.Y., Lin, W.L., Jiang, X.M., Yan, P., Jia, X.F., 2011. Characteristics of
508 atmospheric ammonia over Beijing, China. *Atmospheric Chemistry & Physics*
509 *Discussions* 11, 6139-6151.
- 510 Nowak, J.B., Neuman, J.A., Bahreini, R., Brock, C.A., Middlebrook, A.M., Wollny,
511 A.G., Holloway, J.S., Peischl, J., Ryerson, T.B., Fehsenfeld, F.C., 2010. Airborne
512 observations of ammonia and ammonium nitrate formation over Houston, Texas.
513 *Journal of Geophysical Research Atmospheres* 115, -.
- 514 Pan, Y., Tian, S., Zhao, Y., Zhang, L., Zhu, X., Gao, J., Huang, W., Zhou, Y., Song, Y.,
515 Zhang, Q., 2018. Identifying ammonia hotspots in China using a national observation
516 network. *Environmental Science & Technology* 52, acs.est.7b05235.
- 517 Pandolfi, M., Amato, F., Reche, C., Alastuey, A., Otjes, R.P., Blom, M.J., Querol, X.,
518 2012. Summer ammonia measurements in a densely populated Mediterranean city.
519 *Atmospheric Chemistry & Physics Discussions* 12, 7557-7575.
- 520 Ru-Jin, H., Yanlin, Z., Carlo, B., Kin-Fai, H., Jun-Ji, C., Yongming, H., Daellenbach,
521 K.R., Slowik, J.G., Platt, S.M., Francesco, C., 2014. High secondary aerosol
522 contribution to particulate pollution during haze events in China. *Nature* 514, 218-222.
- 523 Su, H., Cheng, Y., Zheng, G., Wei, C., Mu, Q., Zheng, B., Wang, Z., Zhang, Q., He, K.,
524 Carmichael, G., 2016. Reactive nitrogen chemistry in aerosol water as a source of
525 sulfate during haze events in China. *Science Advances* 2, e1601530-e1601530.
- 526 Sutton, M.A., Dragosits, U., Tang, Y.S., Fowler, D., 2000. Ammonia emissions from
527 non-agricultural sources in the UK - source testing results. *Atmospheric Environment*
528 34, 855-869.
- 529 Ti, C., Gao, B., Luo, Y., Wang, X., Wang, S., Yan, X., 2018. Isotopic characterization
530 of $\text{NH}_x\text{-N}$ in deposition and major emission sources. *Biogeochemistry* 138, 85-102.
- 531 Tian, M., Wang, H.B., Chen, Y., Zhang, L.M., Shi, G.M., Liu, Y., Yu, J.Y., Zhai, C.Z.,
532 Wang, J., Yang, F.M., 2017. Highly time-resolved characterization of water-soluble
533 inorganic ions in PM 2.5 in a humid and acidic mega city in Sichuan Basin, China.
534 *Science of the Total Environment* 580, 224-234.
- 535 Vitousek, P.M., Mooney, H.A., Lubchenco, J., Melillo, J.M., 2008. Human
536 Domination of Earth's Ecosystems, in: Marzluff, J.M., Shulenberger, E., Endlicher,
537 W., Alberti, M., Bradley, G., Ryan, C., Simon, U., ZumBrunnen, C. (Eds.), *Urban*

- 538 Ecology: An International Perspective on the Interaction Between Humans and Nature.
539 Springer US, Boston, MA, pp. 3-13.
- 540 Walters, W.W., Chai, J., Hastings, M.G., 2019. Theoretical Phase Resolved Ammonia–
541 Ammonium Nitrogen Equilibrium Isotope Exchange Fractionations: Applications for
542 Tracking Atmospheric Ammonia Gas-to-Particle Conversion. *ACS Earth and Space*
543 *Chemistry* 3, 79-89.
- 544 Walters, W.W., Hastings, M.G., 2018. Collection of Ammonia for High
545 Time-Resolved Nitrogen Isotopic Characterization Utilizing an Acid-Coated
546 Honeycomb Denuder. *Anal Chem* 90, 8051-8057.
- 547 Wang, J., Xie, P.H., Qin, M., Ling, L.Y., Cong-Lei, Y.E., Liu, J.G., 2012. Study on the
548 Measurement of Ambient Ammonia in Urban Area Based on Open-Path DOAS
549 Technique. *Spectroscopy & Spectral Analysis* 32, 476-480.
- 550 Wang, W., Wang, S., Xu, J., Zhou, R., Shi, C., Zhou, B., 2016. Gas-phase ammonia and
551 PM_{2.5} ammonium in a busy traffic area of Nanjing, China. *Environmental Science &*
552 *Pollution Research* 23, 1691-1702.
- 553 Wentao, W., Narumol, J., Jill, S., Yuling, J., Shu, T., Tian-Wei, Y., Dashwood, R.H.,
554 Wei, Z., Xuejun, W., Simonich, S.L.M., 2011. Concentration and photochemistry of
555 PAHs, NPAHs, and OPAHs and toxicity of PM_{2.5} during the Beijing Olympic Games.
556 *Environmental Science & Technology* 45, 6887-6895.
- 557 Williams, P.T., 2005. *Waste Treatment and Disposal*, Second Edition.
- 558 Xiao, H.-W., Xiao, H.-Y., Long, A.-m., Wang, Y.-L., 2012. Who controls the monthly
559 variations of NH₄⁺ nitrogen isotope composition in precipitation? *Atmospheric*
560 *Environment* 54, 201-206.
- 561 Xin, H., Yu, S., Li, M., Li, J., Huo, Q., Cai, X., Tong, Z., Min, H., Zhang, H., 2012. A
562 high-resolution ammonia emission inventory in China. *Global Biogeochemical Cycles*
563 26, -.
- 564 Xu, W., Luo, X.S., Pan, Y.P., Zhang, L., Tang, A.H., Shen, J.L., Zhang, Y., Li, K.H.,
565 Wu, Q.H., Yang, D.W., 2015. Quantifying atmospheric nitrogen deposition through a
566 nationwide monitoring network across China. *Atmospheric Chemistry and*
567 *Physics*, 15, 21(2015-11-09) 15, 18365-18405.
- 568 Yin, S.S., Zheng, J.Y., Zhang, L.J., Zhong, L.J., 2010. Anthropogenic Ammonia
569 Emission Inventory and Characteristics in the Pearl River Delta Region. *Environmental*
570 *Science* 31, 1146-1151.
- 571 Young, L.H., Li, C.H., Lin, M.Y., Hwang, B.F., Hsu, H.T., Chen, Y.C., Jung, C.R.,
572 Chen, K.C., Cheng, D.H., Wang, V.S., 2016. Field performance of a semi-continuous
573 monitor for ambient PM_{2.5} water-soluble inorganic ions and gases at a suburban site.
574 *Atmospheric Environment* 144, 376-388.
- 575 Zhang, X., Y., CAO, J., J., LI, L., M., ARIMOTO, CHENG, 2002. Characterization of
576 atmospheric aerosol over XiAn in the South Margin of the Loess Plateau, China.
577 *Atmospheric Environment* 36, 4189-4199.

- 578 Zhang, L., Altabet, M.A., Wu, T., Hadas, O., 2007. Sensitive Measurement of NH_4^+
579 $^{15}\text{N}/^{14}\text{N}$ ($\delta^{15}\text{N}_{\text{NH}_4^+}$) at Natural Abundance Levels in Fresh and Saltwaters. *Analytical*
580 *Chemistry* 79, 5297-5303.
- 581 Zheng, J., Yan, M., Chen, M., Qi, Z., Lin, W., Khalizov, A.F., Lei, Y., Zhen, W., Xing,
582 W., Chen, L., 2015. Measurement of atmospheric amines and ammonia using the high
583 resolution time-of-flight chemical ionization mass spectrometry. *Atmospheric*
584 *Environment* 102, 249-259.
- 585
- 586 Hironori Yabu, Chikako Sakai, Tomoko Fujiwara, Naomichi Nishio, Yutaka
587 Nakashimada, Thermophilic two-stage dry anaerobic digestion of model garbage with
588 ammonia stripping, *Journal of Bioscience and Bioengineering*, 2011, 312-319.
- 589
- 590 Damme M V, Clarisse L, Whitburn S, et al. Industrial and agricultural ammonia point
591 sources exposed. *Nature*, 2018, 564(7734).
- 592 Xiurui Guo, Zhilan Ye, Dongsheng Chen, et al. Prediction and mitigation potential of
593 anthropogenic ammonia emissions within the Beijing–Tianjin–Hebei region, China,
594 *Environmental Pollution*, 2019, 113863, ISSN 0269-7491.
- 595 Nebila Lichiheb, LaToya Myles, Erwan Personne et al. Implementation of the effect
596 of urease inhibitor on ammonia emissions following urea-based fertilizer application
597 at a *Zea mays* field in central Illinois: A study with SURFATM- NH_3 model,
598 *Agricultural and Forest Meteorology*, Volumes 269–270, 2019, ISSN 0168-1923.
- 599 Wen Xu, Xuejun Liu, Lei Liu, et al. Impact of emission controls on air quality in
600 Beijing during APEC 2014: Implications from water-soluble ions and carbonaceous
601 aerosol in $\text{PM}_{2.5}$ and their precursors, *Atmospheric Environment*, Volume 210, 2019,
602 Pages 241-252, ISSN 1352-2310.
- 603 Zhongyi Zhang, Yang Zeng, Nengjian Zheng, et al. Fossil fuel-related emissions were
604 the major source of NH_3 pollution in urban cities of northern China in the autumn of
605 2017, *Environmental Pollution*, Volume 256, 2020, 113428, ISSN 0269-7491.
- 606 Elliott E M , Yu Z , Cole A S , et al. Isotopic advances in understanding reactive
607 nitrogen deposition and atmospheric processing. *The Science of the Total*
608 *Environment*, 2019, 662(20):393-403.
- 609 M.J Roadman, J.R Scudlark, J.J Meisinger, et al. Validation of Ogawa passive
610 samplers for the determination of gaseous ammonia concentrations in agricultural
611 settings. *Atmospheric Environment*, 2003, 37(17):2317-2325
- 612 S. Générmont, Cellier P . A mechanistic model for estimating ammonia volatilization

613 from slurry applied to bare soil. *Agricultural and Forest Meteorology*, 1997,
614 88(1-4):0-167.

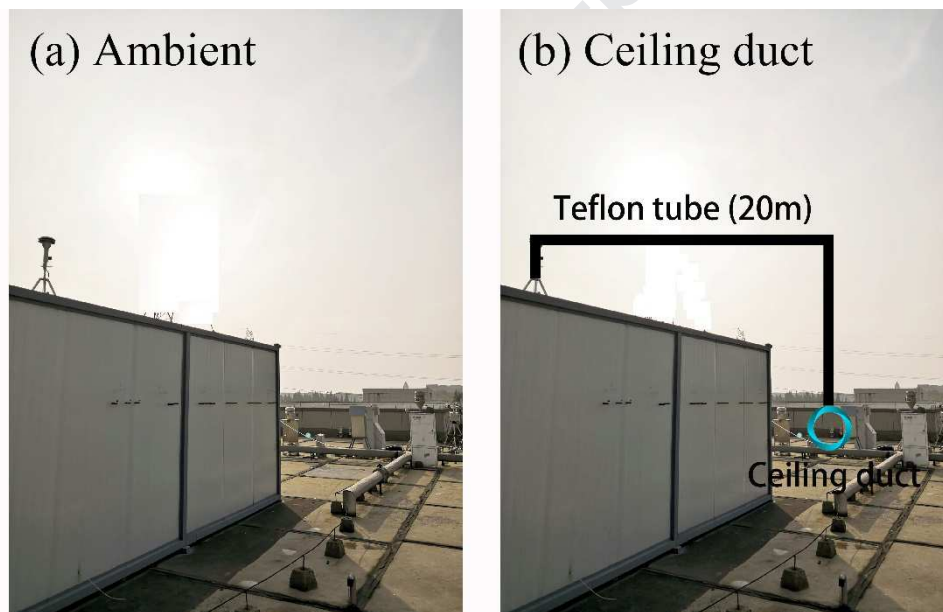
615 Paul A. Roelle, Viney P. Aneja, Characterization of ammonia emissions from soils in
616 the upper coastal plain, North Carolina, *Atmospheric Environment*, 2002, 1087-1097.

617 Beuning J D , Pattey E , Edwards G , et al. Improved temporal resolution in
618 process-based modelling of agricultural soil ammonia emissions[J]. *Atmospheric*
619 *Environment*, 2008, 42(14):3253-3265.

620 Process Modeling of Ammonia Volatilization from Ammonium Solution and Manure
621 Surfaces: A Review with Recommended Models[J]. *Transactions of the ASABE*,
622 2009, 52(5):1707-1720.

623 Kohl D H , Shearer G B , Commoner B . Fertilizer Nitrogen: Contribution to Nitrate
624 in Surface Water in a Corn Belt Watershed[J]. *Science*, 1971, 174(4016):1331-1334.

625



626

627

Figure S1. Field picture of instruments set-up on the rooftops of WDL.

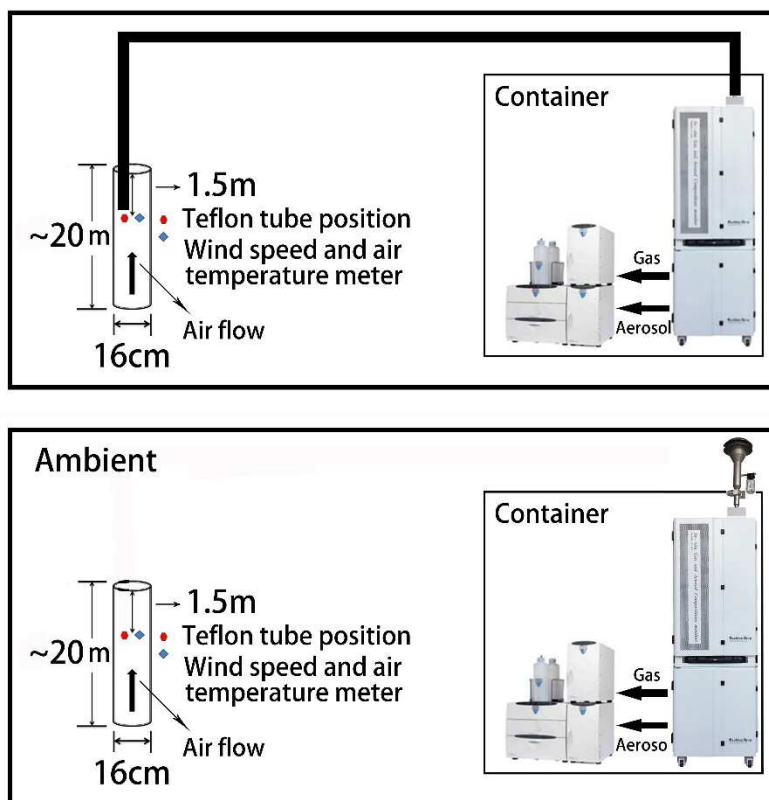


Figure S2. A sketch of the collection between ceiling duct and IGAC instrument.

Highlights

1. We performed highly time-resolved measurements of NH_3 concentrations and auxiliary parameters in the ceiling duct of a typical building
2. Temperature is the key factor in controlling NH_3 emissions from human excreta.
3. Here we report the $\delta^{15}\text{N-NH}_3$ measured from ceiling duct collected directly.

Journal Pre-proof

Declaration of interests

The authors declare that they have no known competing financial interests or personal relationships that could have appeared to influence the work reported in this paper.

The authors declare the following financial interests/personal relationships which may be considered as potential competing interests:

Journal Pre-proof